ELSEVIER

Agricultural and Forest Meteorology 108 (2001) 281–292

AGRICULTURAL AND FOREST METEOROLOGY

www.elsevier.com/locate/agrformet

A new approach to infrared thermometry

John M. Baker [a,*], John M. Noman [b], Atsushi Kano [c]

[a] *USDA-ARS, Department of Soil, Water and Climate, University of Minnesota, 1991 Upper Buford Circle, St. Paul, MN 55108, USA*
[b] *Department of Soil Science, University of Wisconsin–Madison, Madison, WI, USA*
[c] *Faculty of Agriculture, Shizuoka University, Shizuoka, Japan*

Received 17 November 2000; received in revised form 08 April 2001; accepted 12 April 2001

Abstract

Surface temperature is a crucial variable linking surface–atmospheric energy exchange, but it is difficult to measure accurately. Remote measurement by infrared (IR) thermometry is often the only viable choice, but is plagued by problems that limit its absolute accuracy. Primary among these are calibration shifts and an inability to eliminate or properly account for the influence of detector temperature on the measurement. We have developed a new approach that avoids these and other difficulties by making the measurement differentially, essentially providing continuous calibration. The system uses a conventional infrared thermometer (IRT) coupled to a rotary actuator so that its field of view can be periodically switched from the target of interest to a blackbody cavity, whose temperature is controlled with a Peltier block/controller board assembly and measured with carefully calibrated thermocouples. The blackbody temperature is controlled so that the detector output is the same when viewing the blackbody as it is when viewing the target surface. When this condition is satisfied the blackbody temperature and the brightness temperature of the target surface are equal, i.e. the thermal radiation emanating from each is the same.

A prototype instrument, using a conventional IRT as the detector, was built and tested in the laboratory by using it to measure the surface temperature of a mineral oil reservoir that was cycled over a range of temperatures and independently monitored with calibrated thermocouples. Over a 24°C temperature range, the mean absolute error of the instrument was 0.04°C, and a regression against thermocouple-measured oil temperature yielded a slope of 1.002, intercept of −0.015°C, and r^2 of 0.99998, substantially better than the performance of a conventional IRT subjected to the same tests. A field instrument was also built, based on these principles but with smaller components for lower power consumption and lower cost. In an important departure, it uses two IR detectors and a modified switching/control algorithm that provides improved dynamic response while maintaining the accuracy of the prototype. We conclude that continuously-calibrated IR thermometry (CC-IRT) is a viable means for improving the accuracy of radiometric temperature measurement.

Keywords: Infrared thermometry; Surface temperature; Blackbody cavity

1. Introduction

Surface temperature measurements have many applications in the physical and environmental sciences. Surface temperature is the key variable coupling the radiative, conductive, and convective transport processes that comprise the energy balance of an exposed surface. Hence, surface temperature measurements have been used as a yardstick to assess the output of soil/plant/atmosphere models (Baker et al., 1996), as inputs to models of surface fluxes (Kustas and Norman, 1997), and as indicators of crop water stress (Idso, 1981). Sea surface temperature measurements are assuming increasing importance for

* Corresponding author. Tel.: +1-612-625-4249; fax: +1-651-649-5175.
E-mail address: jbaker@soils.umn.edu (J.M. Baker).

0168-1923/01/$ – see front matter © 2001 Published by Elsevier Science B.V.
PII: S0168-1923(01)00248-9

medium-range climatological forecasts (Lau, 1997) and globally-averaged surface temperature trends are potentially a critical piece of evidence in the ongoing dialogue regarding the extent and intensity of human impact on global climate (Kerr, 1998). Many more applications for surface temperature data will likely be proposed with the increasing availability of radiometric observations from satellites. However, ground-based measurements will remain important, both for calibration and correction of data from remote platforms and for the many instances where satellite data are unsuitable (e.g. insufficient spatial or temporal resolution) or unavailable (e.g. under cloudy conditions).

Unfortunately, surface temperature is difficult to measure with the accuracy, resolution, and stability required for many potential applications. Temperature sensors such as thermocouples that depend on attainment of thermal equilibrium with a surface via conductive or convective heat transfer are problematic because they require intimate contact with the surface, which affects the local surface energy balance and thus temperature (Fuchs, 1990). The small sampling area of such sensors can also be an issue under circumstances where it is desirable to obtain a temperature measurement that integrates the effects of spatial heterogeneity. Furthermore, such sensors are themselves affected by radiant energy exchange that can cause their temperature to differ from the surrounding surface. Infrared (IR) thermometry is an attractive alternative that avoids these problems by making non-contact surface temperature measurement, and it has become the method of choice for many applications. Indeed, in vegetative canopies where individual leaves have a range of temperatures, IR thermometry may be the only practical way of measuring "surface" temperature. However, IR thermometry suffers from its own set of limitations.

2. Theory

The spectral distribution of radiance from a perfect emitter, or blackbody, is given by Planck's law (Serway, 1986)

$$I(\lambda, T) = \frac{2\pi hc^2}{\lambda^5\{\exp(hc/\lambda kT) - 1\}} \quad (1)$$

In this expression, T is absolute temperature, c the speed of light in a vacuum, k the Boltzmann constant (1.38×10^{-23} J/K), and h the empirical Planck's constant, found to have a value of 6.626×10^{-34} J s. The outward flux of thermal radiation from a blackbody at temperature T is thus

$$R = \int_{4\pi}\int_{0}^{\infty} I(\lambda, T)\, \mathrm{d}\lambda\, \mathrm{d}\Omega \quad (2)$$

Evaluation of this integral for a Lambertian surface produces the Stefan–Boltzmann equation

$$R = \sigma T^4 \quad (3)$$

where σ is the Stefan–Boltzmann constant, $5.67 \times 10^{-8}\,\mathrm{W\,m^{-2}\,K^{-4}}$. Thus, a measurement of R is sufficient for determining the surface temperature of a blackbody as

$$T = \left(\frac{R}{\sigma}\right)^{1/4} \quad (4)$$

Unfortunately, nearly all surfaces are imperfect emitters, or graybodies, for which the problems in estimating surface temperature from radiometric measurements become more complicated. Extracting the true radiometric surface temperature then requires knowledge of surface emissivity as a function of both temperature and wavelength, and incident radiation as a function of wavelength. These issues are beyond the scope of this manuscript; here we focus solely on the problems associated with accurate measurement of the surface temperature of a blackbody. For graybodies, the results provide an accurate means for measuring brightness temperature, T_b, which is the temperature at which a blackbody would have the same radiance (Norman and Becker, 1995).

A fundamental problem with IR thermometry is that everything emits thermal radiation, including the internal surface of any IRT. As a consequence, even when an IRT is aimed at a blackbody, the radiance reaching its detector does not depend solely on the temperature of the target at which it is pointed, but also on the temperature of the IRT itself. In some instruments, compensation is accomplished by chopping the optical beam, alternately exposing the detector to radiation from the target and radiation reflected from the internal walls of the instrument, then measuring the difference in detector output. In general, the internal

cavity of an IRT is not of uniform temperature, so the detector averages over the internal cavity as well as the chopper itself (because it does not have an emissivity of zero). Clearly, a temperature measurement inside of the instrument may have a different relation to the average cavity temperature depending on operating conditions, so accuracies of 0.1°C generally are not achievable. When thermopile detectors are used to sense the IR signal, the temperature of the reference side of the thermopile will not be the same as the internal cavity temperature, and the thermopile reference may not even maintain a constant offset from the cavity temperature at the 0.1°C level of accuracy. Presumably because mechanical choppers increase the cost and complexity of IRTs and because they are prone to eventual mechanical failure, many instruments do not use them, relying instead on 'electronic chopping', i.e. internal temperature measurements coupled with hardware or software compensation.

The 4000 series IRTs manufactured by Everest Interscience (Tucson, AZ) have received considerable use in environmental biophysics. They have been manufactured in a variety of configurations, including both mechanically and electronically chopped versions, versions with polynomial calibrations, and versions with linearized output. Some models have included a separate output signal that allows the user to directly measure internal temperature, while others apparently include circuitry that compensates for measured internal temperature without troubling the end user. A somewhat confusing picture thus emerges from reported results. Kalma and Alksnis (1988) examined a model 4000 that provided separate signal outputs for detector temperature and thermopile output. They found that the factory supplied polynomial equation for target (surface) temperature produced significant errors, but that the detector temperature measurement was accurate, and that the sensor produced much improved estimates of target temperature when calibrated in terms of the fourth power temperature difference between target and detector. Rapier and Michael (1996) used a later version of the same instrument, the 4000A, which is mechanically chopped, but apparently does not provide detector temperature as an output, instead reading that information with an embedded circuit that also digests the thermopile output and produces a linearized dc voltage (100 mV/°C). They calibrated several sensors periodically over a 12-month period while they were otherwise being used to monitor sea surface temperatures, and concluded that the instruments drift sufficiently that they must be recalibrated on a regular basis. Also implicit in their results is the conclusion that the factory-set calibration is not suitable for maximum accuracy.

Unfortunately, frequent recalibration of a field instrument is not always possible. Furthermore, such a protocol would not solve the fundamental problem of sensitivity to detector temperature. To address these problems and limitations, we have taken a new approach, perhaps best described as continuously-calibrated IR thermometry (CC-IRT). The fundamental premise is that if the IRT can be routinely switched between viewing the target and viewing a blackbody without changing its temperature, and the blackbody can then be heated or cooled until the detector produces the same output signal in both positions, then the temperature of the blackbody, which can be accurately measured by other means, is the same as the brightness temperature of the target. This eliminates the influence of detector temperature and essentially provides continuous calibration.

To test this approach, we first constructed a laboratory prototype, using a commercially available IRT and various parts either scavenged from previous projects or bought at the local hardware store. After tests established the viability of the concept, we designed, built, and tested a system suitable for field research applications. The prototype is only described with sufficient verbiage to communicate how it worked, but the final field version is presented in complete detail.

3. Materials and methods

3.1. Thermocouple calibration

The absolute accuracy of a CC-IRT can be no better than the absolute accuracy with which the temperature of its reference cell (blackbody) can be independently measured. The thermocouple wire and the thermocouple measurement/reference temperature system (23X datalogger, Campbell Scientific, Logan, UT) used in this project were calibrated prior to the experiment. The standard for comparison was a precision platinum resistance thermometer, PRT (Model S7929, Minco, Minneapolis, MN). The PRT is measured in a 4-wire

half-bridge, the output of which provides a ratio of PRT resistance to that of a 100 Ω precision resistor. A 15-order polynomial relates this ratio to temperature. Immediately before the comparison, the PRT was sent back to the factory for recalibration against NBS-traceable standards. Resolution is determined by the bit resolution of the datalogger used to make the ratiometric voltage measurements; in our case it was of the order of 0.018°C.

For the thermocouple calibration, three junctions were made: 0.07 mm reference-grade chromel-constantan, 20 gauge extension-grade chromel-constantan, and 20 gauge extension-grade copper-constantan (all from Omega Inc., Stamford, CT). The three junctions were strapped to the PRT probe with cable ties and the bundle was then immersed in water in a PVC cylinder, 15 cm in diameter and 30 cm high. A coil of copper tubing encircling the cylinder on the inner wall was connected to a temperature controlled water bath, the temperature of which was changed by 2°C every 2 h, cycling between 5 and 35°C several times. The calibration was repeated twice with other dataloggers (both CR7X loggers, Campbell Scientific).

3.2. Prototype instrument

A portable IRT (Model 4000.4 GL, Everest Interscience, Tucson, AZ) was coupled to a stepping rotary solenoid (Lucas Ledex, Vandalia, OH) so that its field of view could be routinely switched between the surface of interest and a temperature-controlled blackbody. The IRT, an electronically chopped model with a passband of 9.8–11.4 μm, had been calibrated and adjusted at the factory to provide a linear output of 10 mV/°C, with a specified accuracy of ±0.5°C. The blackbody was made from an aluminum block with outer dimensions of 28 mm × 28 mm × 32 mm in length, with a black, anodized inner surface. Anodized aluminum has a reported emissivity of approximately 0.94. Given this value and the dimensions of the cavity, the blackbody should have an effective emissivity of at least 0.995 (Sparrow et al., 1962). The bottom of the cavity had a small chromel-constantan thermocouple (0.07 mm diameter) attached to it. The blackbody was insulated with styrofoam and attached to an aluminum heat sink with a Peltier block sandwiched between them. A controller board taken from a dewpoint generator (LiCor, Lincoln, NE) provided power to the Peltier block. It adjusted the polarity and the power input to heat or cool as needed to balance a setpoint voltage and a control voltage. The setpoint voltage was proportional to the signal from the IRT when it was viewing the target, while the control voltage was proportional to the signal from the IRT while viewing the blackbody. A datalogger (Campbell Scientific, Logan, UT) was used to read the voltage signals from the IRT and the blackbody thermocouple, provide signals to the controller board, and to initiate the movement of the stepping solenoid.

The solenoid was mounted to an aluminum baseplate to which an aluminum cone was also mounted, such that one of the 12 positions of the solenoid aims, the IRT directly downward through the cone. The blackbody/heat sink assembly was mounted to the baseplate at a 30° angle from the axis of the cone so that one step of the solenoid aligns the field of view of the IRT with the opening in the blackbody cavity. A copper plate, bent at a 30° angle, was attached to both the blackbody cavity and the cone. Each plane has a 2 cm viewing hole centered in a removable square plate, 2.5 cm on each side. A thin piece of foam insulation separates the copper plate from the blackbody.

3.3. Laboratory test of prototype

The prototype was positioned inside a growth chamber so that its viewing cone was directly above a temperature controlled mineral oil reservoir. The reservoir was constructed from a 15 cm diameter PVC end cap, to which an aluminum cone was attached. A coil of copper tubing encircled the inner wall of the end cap and also passed several times around the aluminum cone. Each end was connected by polyethylene tubing to a temperature-controlled water bath, permitting a circulating solution of water and ethylene glycol to control the temperature of both the reflective cone and the mineral oil with which the end cap was filled. The reservoir/cone assembly was wrapped with fiberglass insulation and placed on a magnetic stirring platform to ensure uniform temperature throughout the oil. Mineral oil was used in preference to water because it is non-volatile, eliminating problems associated with condensation on the inner wall of the cone. Chromel-constantan thermocouples were used to measure the temperature of the oil and of the cone.

During the test, the bath temperature was changed by 2°C every hour, cycling between 12 and 36°C. Temperature of the growth chamber for the initial trial was 20 ± 0.50°C. The prototype was operated so that the IRT was switched every two minutes, first viewing the oil reservoir, then the blackbody cavity. The blackbody was controlled to produce the same output voltage from the IRT in both viewing positions. The laboratory test was repeated using the Everest 4000 IRT in conventional mode, and then both calibration tests were repeated at an ambient temperature of 30 ± 0.50°C.

3.4. Field instrument

The field instrument was designed in the spirit of the laboratory prototype, but with some additional criteria.

1. Minimal size and weight.
2. Low power consumption.
3. Improved dynamic response.

Toward these ends, we developed the system shown in Fig. 1. The critical components are two small thermopile IR detectors (Model S60, Dexter Research, Dexter, MI). These face opposite directions in a copper housing that keeps them at the same temperature. The housing is coupled to a shaft that is connected to a rotary servo (Model 514B, Futaba Corp., Schaumburg, IL) of the sort used to move the ailerons on radio-controlled model airplanes. This servo rotates the housing within an outer ring, also of copper, that has two openings. One faces the target of interest while the other faces a blackbody cavity, attached to the ring but with an intervening piece of styrofoam insulation. A Peltier block (Model CP1.0-3l-08L, Melcor Corp., Trenton, NJ) is sandwiched between the back of the blackbody and a copper heat sink that transfers heat between the block and the aluminum outer housing of the entire apparatus. The position of the servo is dictated by the width (length of time) of a 5 VDC pulse, which is supplied by the datalogger using a custom instruction provided by the manufacturer, Campbell Scientific. The Dexter detectors consist of thermopiles in an argon-filled can with a Germanium window that has a bandpass of 8–14 μm. The field of view and sensitivity, mV/(W m^{-2}), are determined by the aperture diameter.

We established the field of view of the instrument by rotating it in 1° increments through a 180° arc, in the center of which was the heated tip of a soldering iron approximately 1 m distant, while measuring the thermopile output at each stop. The calibration of each of the two detectors was determined by measuring their output while viewing a temperature-controlled cavity as its temperature was changed in stepwise fashion over a temperature range from 10 to 35°C.

One of the drawbacks of the prototype was a limited dynamic response. Since it contained a single IRT switched between target and blackbody it could only track a changing surface temperature with frequent switching, increasing the power requirement and the wear and tear on mechanical parts. To avoid this, the field instrument was designed with two detectors, and the control algorithm was modified accordingly. To illustrate how it works, one switching cycle is described. If we begin with detector A viewing the target and detector B viewing the blackbody, just before switching we save the final voltage output of detector A, ζ. This serves as our initial setpoint value, G, after switching. Immediately after switching, we take the initial output from detector B, which is now viewing the target, as α. The output of detector A, which is now viewing the blackbody, is V_{BB}, and the control circuit operates to make V_{BB} equal to the setpoint value. However, to accommodate a changing target temperature, we modify G on the basis of changes in the output of detector B, V_T

$$G = \zeta + (V_T - \alpha)\frac{s_a}{s_b} \tag{5}$$

where s_a/s_b is the ratio of the calibration slopes of the two detectors. The same strategy is followed on subsequent switching with the voltages from the appropriate detector used for α, ζ, V_T, and V_{BB}, and the calibration ratio inverted when detector B is viewing the blackbody. Any error or uncertainty in the detector calibrations only affects the second term in Eq. (5) so as long as $V_T - \alpha$ is small relative to ζ, the effect on the surface temperature measurement will be minimal. In fact, the switching interval can be conditioned on that basis so that whenever $V_T - \alpha$ exceeds some fraction of ζ the detectors will be switched.

The Peltier control circuit used in the field instrument was considerably smaller and less expensive than the one used in the prototype. It uses a simple power

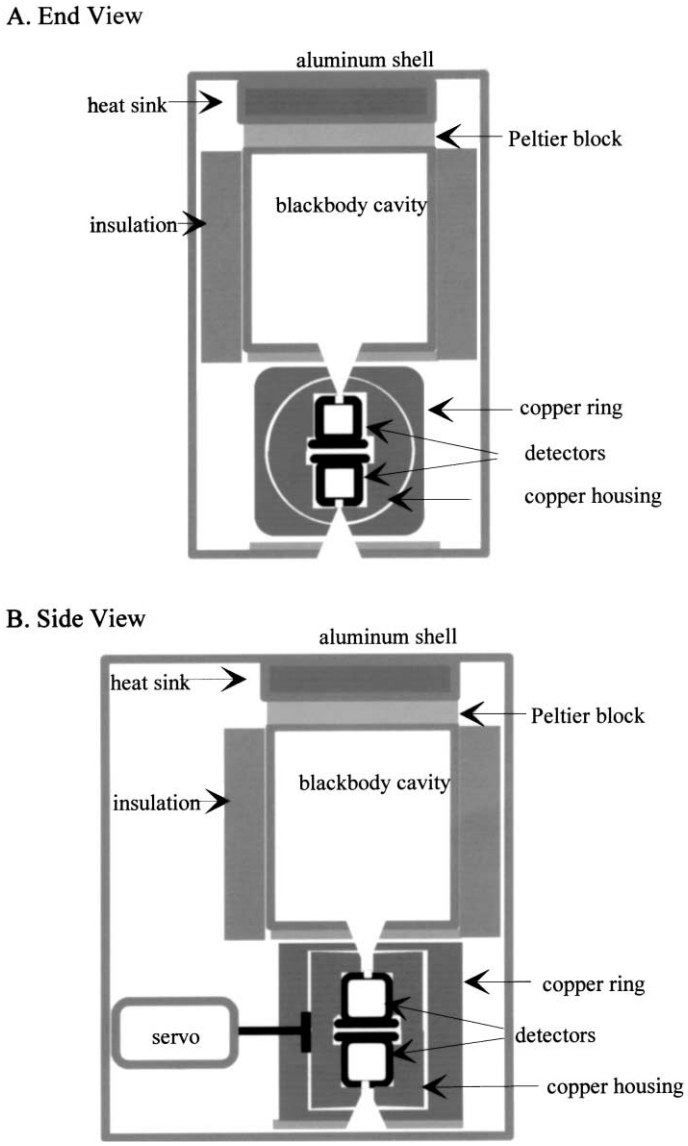

Fig. 1. Schematic of the final (field) version of the CC-IRT. The upper drawing is an end view and the lower drawing is a side view, with respect to the axis of rotation. The servo rotates the two detectors so that one is always viewing the blackbody and one is viewing the target. The drawing is not to scale, but the entire assembly is housed in an electrical box that is 15.2 cm × 10.2 cm × 7.6 cm.

supply (0–10 V, 1 A stabilized power supply kit, Ele Kobo Sakurai, Yono, Japan), a relay to reverse output polarity, and a PID control algorithm programmed into the datalogger to control the magnitude of the output voltage. The algorithm is explained in the Appendix A.

After the detectors had been calibrated to determine s_a/s_b, the instrument was tested by using it to measure the temperature of an anodized aluminum block that was encircled by a copper coil through which fluid from a temperature-controlled water bath could be circulated. Thermocouples in the block monitored

the temperature as it was cycled through a range from 15 to 34°C while its temperature was independently measured by the CC-IRT.

4. Results and discussion

4.1. Thermocouple calibration

The three dataloggers yielded similar results for the reference-grade chromel-constantan thermocouples, with each exhibiting a minimum error of approximately 0.08°C at or near the point where water temperature and reference temperature were the same, and each showing a nonlinear, but small, increase in error as difference between water and air temperature increased (Fig. 2). Results for the extension-grade chromel-constantan are quite different from the reference-grade, but there is good agreement between the two CR7X loggers. The data for the extension-grade copper-constantan, measured by the CR23X are also distinctly different, but all calibrations converge to give errors of approximately 0.08°C in the vicinity of the null temperature difference between water and datalogger (the point at which there is no thermocouple emf). Apparently, the standard used by Campbell Scientific to calibrate its datalogger reference temperature sensors differs from that of Minco to about 0.08°C. On one of the calibration runs the water bath was accidentally set to −5°C; when this error was discovered a slurry of ice had begun to form in the calibration tank. The PRT readings at this time were within 0.02°C of 0, while the thermocouple readings from the logger were about 0.15°C; qualitative evidence that the calibration of the PRT was accurate, and that the 0.08°C offset mentioned earlier may be ascribable to the dataloggers. The increasing error at temperatures farther from the reference (slope error) we tentatively interpret as a discrepancy between the thermocouple emf generated by the chromel/constantan wire and the chromel/constantan standard equation used by the datalogger, possibly due to impurities in the wire. The error was noticeably smaller for the reference-grade wire than for the extension-grade wire. In subsequent work, the 0.08°C offset was subtracted from all thermocouple measurements, but no attempt was made to correct for the apparent nonlinearity in the thermocouple equation,

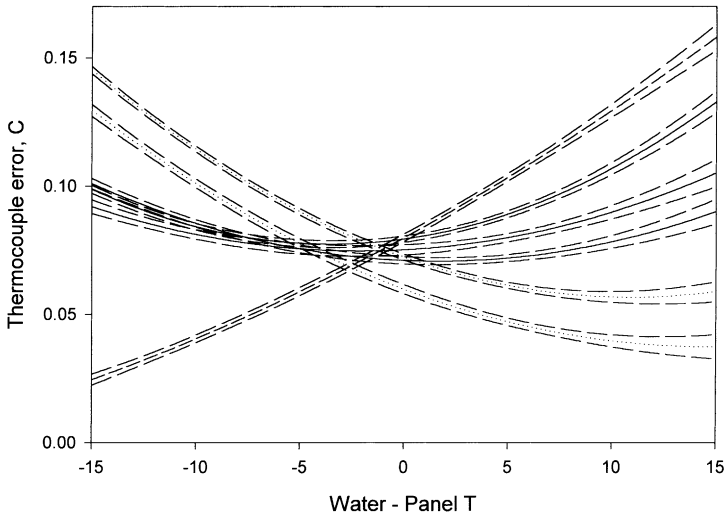

Fig. 2. Thermocouple calibration results. Thermocouples were calibrated against a platinum resistance thermometer. The solid lines represent second order regression fits of data collected with a 0.07 mm reference-grade, chromel-constantan junction read in separate calibration runs by two different CR7X dataloggers and a CR23X datalogger. The dotted lines are second order fits of data from a 20 gauge extension grade chromel-constantan junction with the two CR7X loggers, and the short dashed line is data obtained with a 20 gauge extension-grade copper-constantan junction read by the CR23X logger. The medium dashed lines bracketing each regression represent 95% confidence intervals.

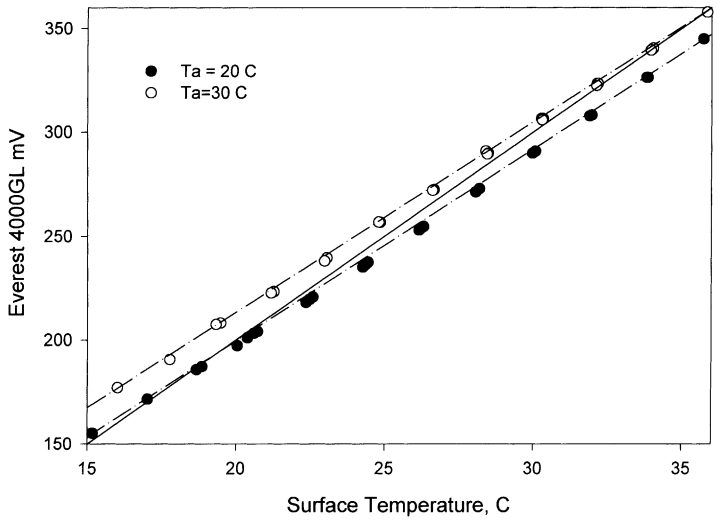

Fig. 3. Laboratory tests of the factory-calibrated Everest 4000 IRT, showing IRT estimates of oil surface temperature against oil temperature measured by chromel-constantan thermocouples. Two test runs were conducted, one with an ambient (detector) temperature of 20°C, and one at 30°C. The solid line is the factory preset calibration of $T_s = 0.1$ mV. Regression results for the two test runs are — at 20°C: $T_{s,Everest} = 0.09252\,(\text{mV}) + 1.226$, $r^2 = 0.996$ and at 30°C: $T_{s,Everest} = 0.09131\,(\text{mV}) + 2.953$, $r^2 = 0.9998$.

since the nonlinearity error for the reference-grade wire is small unless the difference between reference temperature and junction temperature is quite large.

4.2. Conventional IRT evaluation

The laboratory results for the conventional, factory-calibrated IRT are shown in Fig. 3. For each of the two ambient (detector) temperatures, the results are quite linear, but the slopes are disturbingly far from 1.0, and the intercepts are not particularly close to 0. More telling, the results at the two ambient temperatures clearly differ from one another. The solid line in the figure represents the factory calibration. Interestingly, it matches the data well when the target and detector temperatures are the same, both at 20 and 30°C, suggesting that it is a 'best-fit' compromise.

According to the Everest 4000 manual, the instrument is calibrated with a 'preset emissivity' of 0.98, and it has a small screw that should be adjusted for surfaces with emissivities other than 0.98. On some instruments, this screw is covered by a knob and dial so that the user can dial in the correct emissivity. This evidently alters the gain adjustment on the detector output, but it is clear that this cannot adequately account for emissivity, since changes in emissivity have opposite effects on emitted and reflected radiation. This has been stated previously (e.g. Fuchs, 1990), but apparently needs amplification; it makes no sense to put an emissivity adjustment knob on an IRT for environmental use. We tried correcting for the 'preset emissivity' embedded in the factory calibration by using Eq. (6)

$$T_c = \left(\frac{0.98}{\varepsilon_{\text{cavity}}}\right)^{1/4} T_f \tag{6}$$

where T_c is the corrected estimate of brightness temperature and T_f the factory calibration estimate of brightness temperature (both in K). The emissivity of the cavity is estimated to exceed 0.995, particularly since the temperature of the cone above the oilbath was maintained at the same temperature as the oilbath. When this correction was made, the mean absolute error of the factory calibration increased from 0.659 to 1.54°C. Under the circumstances, there appears to be no point in making this correction.

Two additional points are evident: the output of the conventional IRT depends on both detector and target temperature, and as a corollary, no matter how carefully a factory or user calibration is done, subsequent

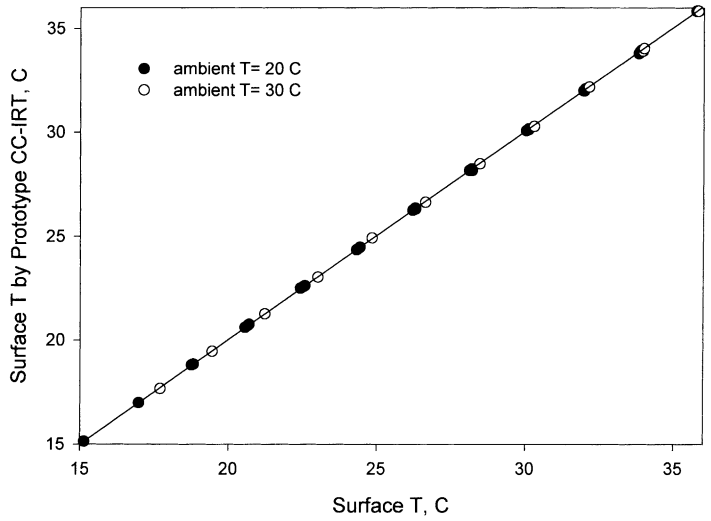

Fig. 4. Laboratory test of the prototype, showing CC-IRT estimates of oil surface temperature against oil temperature measured by chromel-constantan thermocouples. As with the standard Everest 4000 test, two runs were conducted, one at an ambient (detector) temperature of 20°C, and one at 30°C. Regression results for the two test runs are — at 20°C: $T_{s,\text{CC-IRT}} = 1.002\,(\text{T}) - 0.015$, $r^2 = 0.99998$ and at 30°C: $T_{s,\text{CC-IRT}} = 1.001\,(\text{T}) - 0.016$, $r^2 = 0.9999$.

measurements will be in error unless (a) the detector is always kept at the same temperature at which it was calibrated, or (b) detector temperature is measured and included in the calibration and in subsequent brightness temperature determinations.

4.3. Prototype evaluation

The results for the prototype CC-IRT are presented in Fig. 4. They indicate near-perfect agreement between the CC-IRT estimate of oil bath temperature

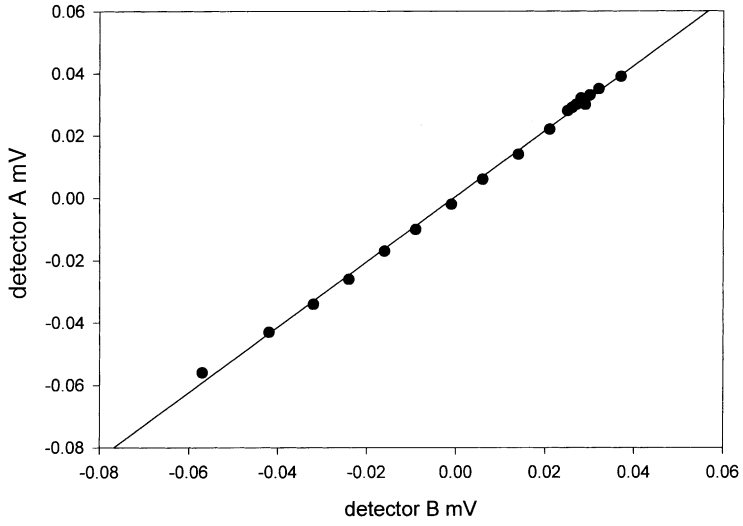

Fig. 5. Comparison of one Dexter IR detector against another. The slope, 1.05, was used in the control algorithm to reduce the frequency of switching the detectors between target and blackbody, as described in the text.

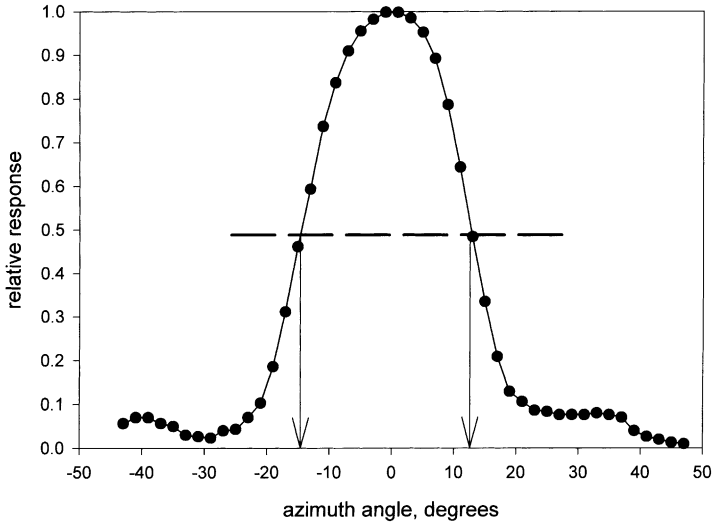

Fig. 6. Determination of the field of view of the CC-IRT. Taking the half-power point as the boundary of the field of view yields a field width of 26°.

and the thermocouple measurements of oil bath temperature. Furthermore, the results from the trial where detector temperature was 30°C are indistinguishable from those collected when it was 20°C, supporting the validity of the concept of CC-IRT.

4.4. Field research instrument evaluation

The calibrations of the two thermopile IR detectors used in the CC-IRT are shown in Fig. 5. The linearity is evident, and the ratio of the two slopes is 1.05. The

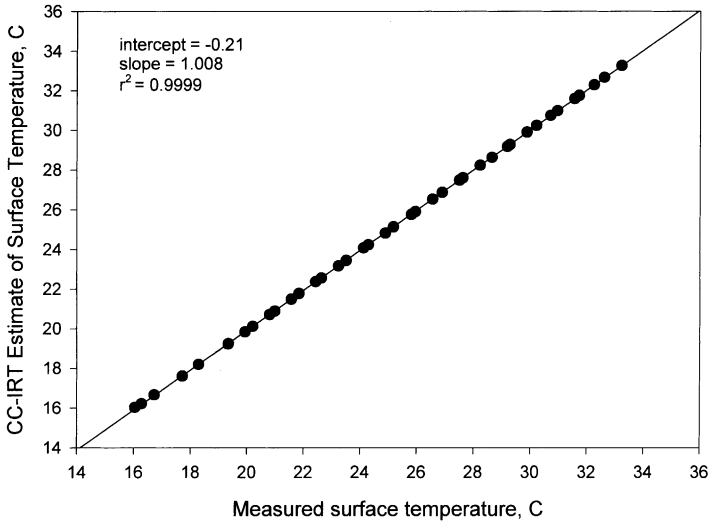

Fig. 7. Test of the accuracy of the CC-IRT. The instrument was used to measure the temperature of an aluminum block. Fluid was circulated from a temperature-controlled water bath through a water jacket surrounding the block to generate a range of block temperatures. The temperature of the block was independently measured by precision-calibrated thermocouples.

field of view of an IRT does not have a distinct cutoff, and hence there is sometimes confusion in terminology. We follow the convention of defining the cutoff at the half-power point. The apertures of the copper housing of the CC-IRT (Fig. 1) were designed to produce a 25° field of view. The laboratory determination, shown in Fig. 6, indicates that the actual field of view is very close to this value. The test of the accuracy of the CC-IRT is shown in Fig. 7. A regression of measured versus actual target temperature has a slope of 1.0008, a correlation coefficient of 0.9999, and a mean absolute error of 0.028°C. Again, this confirms the validity of the general approach, as well as the performance of the new control system in continuously adjusting and maintaining the temperature of the blackbody to keep its thermal exitence equal to that of the target.

5. Conclusions

CC-IRT solves many of the persistent problems of non-contact temperature measurement errors due to sensor temperature effects, errors due to calibration drift, and errors due to the use of the Stefan–Boltzmann equation for a bandpass IRT. It produces results with mean absolute errors of <0.05°C in laboratory tests. While the CC-IRT is somewhat more complicated to use than a conventional IRT, the substantial improvement in performance argues for its use in situations where absolute accuracy matters. The limitation on absolute accuracy in field usage will probably be the accuracy with which emissivity and background radiation are known or can be measured, a formidable remaining barrier to routine, highly accurate remote temperature measurement.

Appendix A

Temperature control of the blackbody

When temperature to be precisely controlled, simple ON–OFF control is not suitable because over- and under-shooting is inevitable.

If variable heating or cooling is possible, temperature can be controlled smoothly by applying output (heating and cooling) proportional to the difference between the desired (set) value and the process (actual) value, Eq. (A.1). This is proportional control (P-control). However, in P-control, there is always a residual error, because when the error is null, there is no control (no output). This residual error, or offset, is given by Eq. (A.2). Note that ON–OFF control is actually a special case of P-control in which the proportional constant is infinite.

$$y = K_\mathrm{p} * e(1), \quad Y = K_\mathrm{p}\phi \tag{A.1}$$

where Y is the control output, K_p is the proportional gain or coefficient and ϕ is the error (=set value–actual value).

$$o = V_\mathrm{s}\frac{1}{1 + K_\mathrm{p}} \tag{A.2}$$

where o is the offset remaining by the P-control and V_s is the set value.

To eliminated of offset, a second control term is introduce that is proportional to the integrated value of the offset. This is integral control (I-control) Eq. (A.3).

$$Y = K_\mathrm{i}\int \phi \,\mathrm{d}t \tag{A.3}$$

where K_i is the coefficient for I-control.

To attain rapid response a third term is included that is proportional to the time derivative of the error. This is derivative control (D-control), Eq. (A.4):

$$Y = K_\mathrm{d}\frac{\mathrm{d}\phi}{\mathrm{d}t} \tag{A.4}$$

where K_d is the coefficient for D-control.

By incorporating P-, I-, and D-controls into the control algorithm both accuracy and rapid dynamic response can be achieved, Eq. (A.5):

$$Y = K_\mathrm{p}\phi + K_\mathrm{i}\int \phi \,\mathrm{d}t + K_\mathrm{d}\frac{\mathrm{d}\phi}{\mathrm{d}t} \tag{A.5}$$

To control the black body temperature of the CC-IRT, we used Eq. (A.5) in a simple datalogger program, empirically adjusting the K-values until we arrived at a set of values that gave us rapid, accurate, and robust control.

References

Baker, J.M., Koskinen, W.C., Dowdy, R.H., 1996. Volatilization of EPTC: simulation and measurement. J. Environ. Qual. 25, 169–177.

Fuchs, M., 1990. Canopy thermal infrared observations. Remote Sens. Rev. 5, 323–333.

Idso, S.B., 1981. Measuring yield-reducing plant water potential depressions in wheat by infrared thermometry remote sensing of plant water stress. Irrig. Sci. 2, 205–212.

Kalma, J.D., Alksnis, H., 1988. Calibration of small infrared surface temperature transducers. Agric. For. Meteorol. 43, 83–98.

Kerr, R.A., 1998. Among global thermometers, warming still wins out. Science 281, 1948–1949.

Kustas, W.P., Norman, J.M., 1997. A two-source approach for estimating turbulent fluxes using multiple angle thermal infrared observations. Water Resour. Res. 33, 1495–1508.

Lau, N.C., 1997. Interactions between global SST anomalies and the midlatitude atmospheric circulation. Bull. Am. Meteorol. Soc. 78, 21–33.

Norman, J.M., Becker, F., 1995. Terminology in thermal infrared remote sensing of natural surfaces. Remote Sens. Rev. 12, 159–173.

Rapier, C.B., Michael, K.J., 1996. The calibration of a small, low-cost thermal infrared radiometer. Remote Sens. Environ. 56, 97–103.

Sparrow, L.M., Albers, L.U., Eckert, E.R.G., 1962. Thermal radiation characteristics of cylindrical enclosures. J Heat Trans. 84, 73–81.

Serway, R.A., 1986. Physics for Scientists and Engineers. Saunders College Publishing, Philadelphia, PA, 1108 pp.